Organic & Biomolecular Chemistry

PAPER

View Article Online
View Journal | View Issue

Cite this: *Org. Biomol. Chem.*, 2017, **15**, 7008

New bioluminescent coelenterazine derivatives with various C-6 substitutions†

Tianyu Jiang,[a] Xingye Yang,[a] Yubin Zhou,[b] Ilia Yampolsky,[c,d] Lupei Du[a] and Minyong Li*[a]

Received 26th June 2017,
Accepted 28th July 2017

DOI: 10.1039/c7ob01554b

rsc.li/obc

A series of new coelenterazine analogs with varying substituents at the C-6 position of the imidazopyrazinone core have been designed and synthesized for the extension of bioluminescence substrates. Some of them display excellent bioluminescence properties compared to DeepBlueC™ or native coelenterazine with both *in vitro* and *in vivo* biological evaluations, thus placing these derivatives among the most ideal substrates for *Renilla* bioluminescence applications.

Introduction

Bioluminescence, as a special form of chemiluminescence, is a natural phenomenon that emits cold light resulting from the reaction catalyzed by the corresponding luciferase in biological systems. The bioluminescent techniques, such as bioluminescence imaging, BRET and dual-luciferase reporter assay system, have drawn more and more attention due to their wide application in examining various biological processes *in vitro* and *in vivo*.[1–5] This method has low background interference compared to fluorescence in that bioluminescence does not require any excitation light source.

Coelenterazine (CTZ), the known widespread luciferin, can be utilized by various marine luciferases from *Renilla*, *Oplophorus*, *Periphylla*, *Gaussia*, *Metridia*, *etc.*, and act as a bound substrate for calcium-binding photoproteins.[6–13] The bioluminescence reaction of coelenterazine is initiated by the binding of O_2 at the C-2 position of the imidazopyrazinone core, which results in the production of the amide anion of coelenteramide in its excited state and CO_2. Then the emission of light is a consequence from the amide anion of coelenteramide in a high energy level relaxing to the ground state.[7,14–16] The coelenterazine–luciferase system is the simplest bioluminescent system consisting of only luciferin and luciferase without any cofactors when compared with systems such as firefly luciferin–luciferase and bacterial bioluminescent systems and others.

A mass of coelenterazine analogues as bioluminescence substrates have consistently appeared since the discovery of coelenterazine.[17–26] It has drawn enormous attention to optimizing the coelenterazine type molecules to obtain substrates that meet ideal criteria, such as bright bioluminescence, long half-decay life, red-shifted emission, high stability and convenient synthesis. The influence of bioluminescence varies with the modification of substitution at the C-2, C-5, C-6 and C-8 positions of the imidazopyrazinone core.[14] Particularly, the optimization of substitution at the C-2 and C-6 positions of the imidazopyrazinone core plays a more important role in improving the bioluminescence properties.[14,27] However, only a few of them have potential to replace the native coelenterazine and to be applied in bioluminescence assay. Some coelenterazine derivatives including coelenterazine h, coelenterazine 400a (DeepBlueC™), coelenterazine f, coelenterazine fcp and coelenterazine hcp were firstly reported by the Cormier lab during the period of 1973–1979.[28,29] Besides, several characteristic coelenterazine analogues have been designed and synthesized in recent years. For example, Promega Corporation developed a new coelenterazine derivative named furimazine that contains a furan group at the C-2 position in 2012.[30] Furimazine is a potent substrate for NanoLuc, an *Oplophorus* luciferase variant also engineered by Promega Corporation. Three coelenterazine analogues with styryl substituents at the C-6 position were reported to serve as substrates for the *Renilla* luciferase mutant in 2014.[20] However, only a few derivatives such as coelenterazine h and DeepBlueC™ that were reported in 1970s have been developed into common substrates that can replace coelenterazine to be used in bioluminescent assays. There are a few substrates that

[a]*Department of Medicinal Chemistry, Key Laboratory of Chemical Biology (MOE), School of Pharmaceutical Sciences, Shandong University, Jinan, Shandong 250012, China. E-mail: mli@sdu.edu.cn; Fax: +86-531-88382076; Tel: +86-531-88382076*
[b]*Center for Translational Cancer Research, Institute of Biosciences and Technology, College of Medicine, Texas A&M University, Houston, TX 77030, USA*
[c]*Shemyakin-Ovchinnikov Institute of Bioorganic Chemistry of the Russian Academy of Sciences, Miklukho-Maklaya, 16/10, Moscow 117997, Russia*
[d]*Pirogov Russian National Research Medical University, Ostrovitianov 1, Moscow 117997, Russia*

†Electronic supplementary information (ESI) available: Other figures, NMR, HPLC and HRMS spectra. See DOI: 10.1039/c7ob01554b

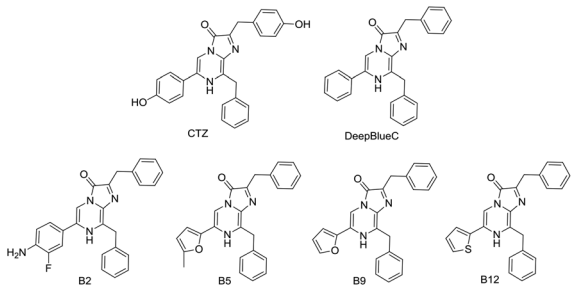

Fig. 1 The known coelenterazine and DeepBlueC™ and new compounds in this article.

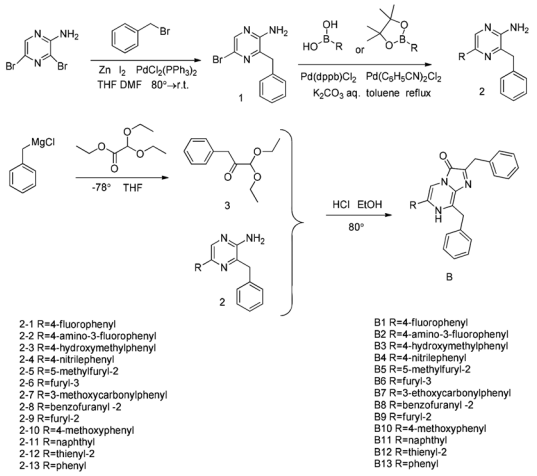

Scheme 1 Synthesis of new derivatives.

are superior to coelenterazine over the last couple of decades. Novel and potent substrates are demanded to fill this gap.

Herein, we designed and synthesized a series of compounds with various substituents at the C-6 position of the imidazopyrazinone core based on coelenterazine 400a (DeepBlueC™) to further investigate the influence of substituents at the C-6 position of the imidazopyrazinone core on the bioluminescence (BL) properties (Fig. 1 and Scheme 1). Particularly, the new compound **B2** is superior to coelenterazine, which is achieved to be the replacement of coelenterazine.

Results and discussion

Bioluminescence properties with *Renilla* luciferase

All new compounds were evaluated with recombinant *Renilla reniformis* luciferase (Rluc) after successful synthesis. As shown in Fig. 2 and Table 1, some of them displayed excellent emission. Compounds **B2**, **B5**, **B9** and **B12** exhibited a much higher intensity than that of DeepBlueC™ in the presence of *Renilla* luciferase. The best substrate **B2** displayed approximately 100-fold stronger emission than the commonly used DeepBlueC™. Compounds **B5** and **B9** exhibited a similar performance in the presence of Rluc, which displayed approximately 20-fold stronger emission compared to DeepBlueC™. Compound **B12** exhibited good performance with approximately 8-fold higher emission than that of DeepBlueC™. Moreover, the BL intensity of **B2** with Rluc was even greater than that of coelenterazine when the concentration of compounds was lower than 1 μM (Fig. 2B). However, compound **B4** exhibited no activity in combination with Rluc. These results reveal that the introduction of the electron-withdrawing group could reduce the bioluminescence. Compounds **B8** with a benzofuranyl group and **B11** substituting a naphthyl group led to less bioluminescence, which indicated that the groups were too large to influence the combination and reaction with luciferase.

Most of our new compounds had red-shifted emission compared to that of DeepBlueC™ (Fig. 2C). The BL spectrum of the **B2**/Rluc pair displayed a 70 nm red-shift in emission when compared with that of DeepBlueC™. Both the **B5**/Rluc pair and the **B8**/Rluc pair had a 30 nm longer BL emission peak than that of DeepBlueC™. However, all of them showed a blue-shift in their BL emission spectra compared to that of native coelenterazine. These findings indicate that the introduction of electron richer groups at the C-6 position which directly contributed to the conjugation degree, could influence the peak emission.

To further assess their kinetic characteristics of bioluminescence, we carried out enzyme kinetic assays and obtained the Michaelis constant K_m, the maximum rate V_{max} and half-decay life by using the GraphPad Prism software. As shown in Table 1 and Fig. S1,† compounds **B2**, **B3** and **B8** had similar K_m values compared to DeepBlueC™. Moreover, most of them (**B2**, **B5**, **B6**, **B7**, **B8**, **B9**, **B10**, **B11** and **B12**) had a higher maximum rate V_{max} in contrast to DeepBlueC™. It is interesting that the maximum rates of **B2**, **B5**, **B9** and **B12** were approaching the V_{max} of native coelenterazine. Furthermore, both **B5** and **B6** had a much longer half-decay life in contrast to DeepBlueC™ and coelenterazine. Therefore the compounds **B2**, **B5**, **B6** and **B9** were the most potential substrates of Rluc when various factors such as kinetic constants, BL intensity and BL peak emission were taken into consideration.

It seemed that the retention or introduction of electron rich groups with suitable sizes at the C-6 position could make great contributions to bioluminescence, which could lead to enhanced bioluminescence intensity, red-shifted maximum wavelength and better kinetic characteristics. The reason is that the polar groups such as an amino group of **B2**, a furanyl containing oxygen atom of **B5** and **B9** and thienyl containing a sulfur atom of **B12** could interact with active-site residues D120, E144, H285 and W121 of Rluc according to the study of Woo *et al.*[13] and Loening *et al.*[31]

In addition, all compounds were evaluated with *Gaussia* luciferase (Table S1†). The BL spectra were similar to that of DeepBlueC™ and coelenterazine. Compound **B2** was still the best one which showed 38-fold stronger emission than that of DeepBlueC™. Compounds **B3**, **B5** and **B8** displayed moderate bioluminescence with *Gaussia* luciferase. However, none of

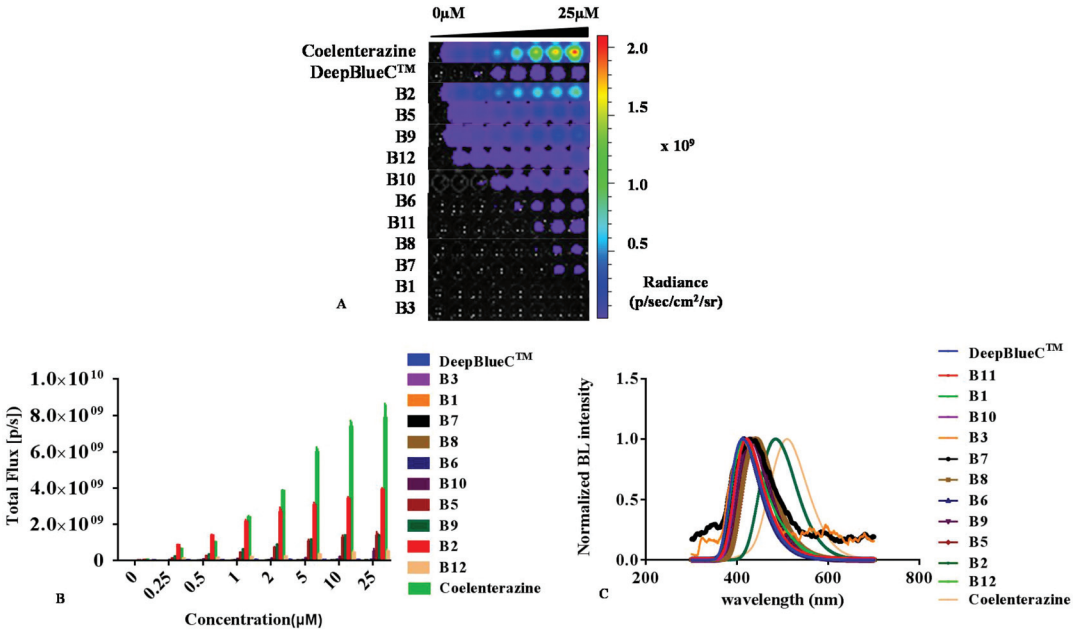

Fig. 2 (A) Bioluminescence imaging of coelenterazine derivatives with *Renilla* luciferase. (B) The comparison of bioluminescence intensities of new derivatives and DeepBlueC™ and coelenterazine at various concentrations with *Renilla* luciferase. (C) Bioluminescence spectra of new derivatives and DeepBlueC™ and coelenterazine with *Renilla* luciferase. BL spectra were obtained with an F-2500 FL spectrophotometer with a response time of 2 s.

Table 1 Bioluminescence properties of all compounds with Renilla luciferase

Compounds	Emission (nm)	Half life[a] (s)	K_m [b] (μM)	V_{max} [b] (s/p)	Intensity (1 μM)%
DeepBlueC™	411	42.2	0.6 ± 0.1	$(3.9 \pm 0.1) \times 10^7$	100
Coelenterazine	509	63.7	2.8 ± 0.2	$(9.0 \pm 0.2) \times 10^9$	9634
B1	417	35.5	1.6 ± 0.2	$(5.4 \pm 0.2) \times 10^6$	9
B2	484	24.7	0.9 ± 0.2	$(3.8 \pm 0.1) \times 10^9$	8645
B3	412	2.80	0.7 ± 0.1	$(2.8 \pm 0.1) \times 10^6$	7
B4	N.A.	N.A.	N.A.	N.A.	N.A.
B5	440	399	2.9 ± 0.2	$(1.7 \pm 0.0) \times 10^9$	1695
B6	415	421	2.0 ± 0.1	$(4.0 \pm 0.1) \times 10^7$	56
B7	428	31.9	3.6 ± 0.2	$(1.7 \pm 0.0) \times 10^7$	15
B8	440	74.6	0.9 ± 0.0	$(2.9 \pm 0.0) \times 10^7$	64
B9	430	6.2	1.8 ± 0.1	$(1.6 \pm 0.0) \times 10^9$	2412
B10	422	26.8	1.1 ± 0.2	$(1.6 \pm 0.1) \times 10^8$	311
B11	420	6.6	1.3 ± 0.2	$(2.2 \pm 0.1) \times 10^7$	40
B12	428	9.91	4.9 ± 0.6	$(8.6 \pm 0.3) \times 10^8$	764

[a] BL half-life was calculated using GraphPad Prism software and taken advantage of the values when compounds were 25 μM. [b] Michaelis constant K_m and maximum rate V_{max} were estimated with the Michaelis–Menten kinetics equation using GraphPad Prism software. The values are shown by means ± SD of three independent assays performed in triplicate.

them was superior to native coelenterazine in the presence of *Gaussia* luciferase. Though most of them had lower K_m, their V_{max} values were inferior to that of native coelenterazine. The results disclosed that the substituents at the C-2 position play a major role in the binding of *Gaussia* luciferase. Moreover, the introduction of the larger size of electron rich substituents could promote the BL emission with *Gaussia* luciferase. The chemiluminescence spectra and fluorescence spectra of all new compounds were also measured as displayed in Table S2.†

Bioluminescence imaging *in cellulo*

Subsequently, we further evaluated their BL properties *in cellulo* with a series of assays taking advantage of ES-2 cells expressing *Renilla* luciferase (ES-2-Rluc). Their BL intensity is depicted in Fig. 3. Compounds **B2**, **B5**, **B6**, **B9** and **B12** are superior to DeepBlueC™ in BL emission in the cellular level. In brief, they all exhibited good performance in the cell concentration-dependent assay (Fig. 4). What's more, it is evident that compound **B2** could emit much stronger bioluminescence

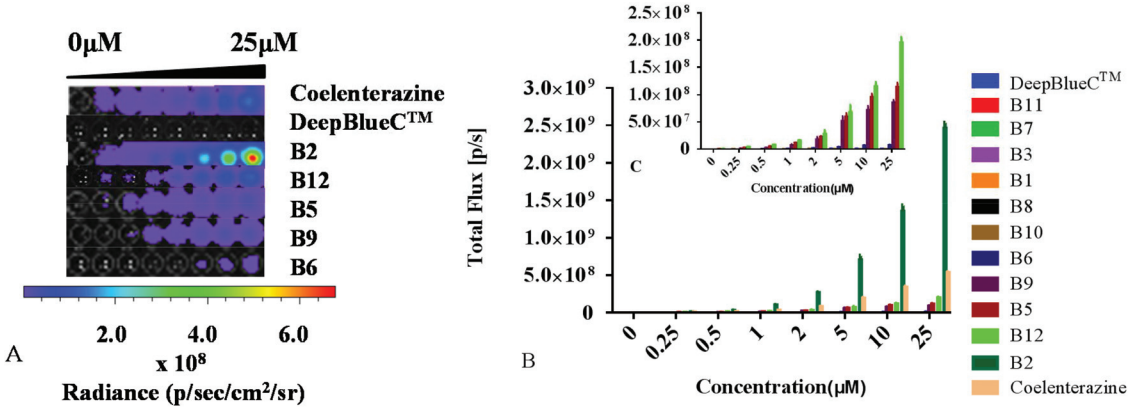

Fig. 3 (A) Bioluminescence imaging of parts of coelenterazine derivatives *in cellulo*; (B) the comparison of bioluminescence intensities of new derivatives and DeepBlueC™ and coelenterazine in ES-2 cells expressing *Renilla* luciferase (Rluc) at various concentrations; (C) parts of compounds that showed bioluminescence *in cellulo*.

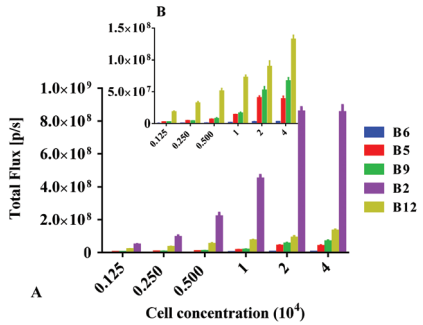

Fig. 4 The comparison of bioluminescence intensities of new derivatives in ES-2 cells expressing *Renilla* luciferase (Rluc) at various cell concentrations (×10⁴): (A) potent compounds that displayed bioluminescence at various cell concentrations; (B) part amplification of graph A.

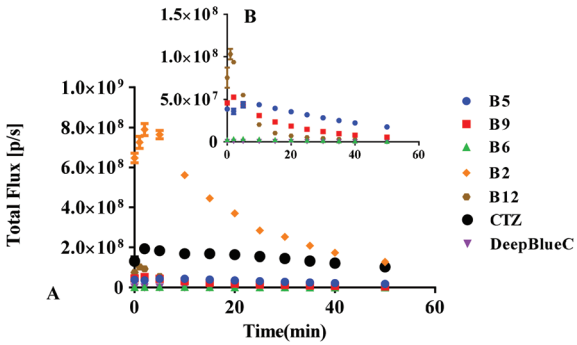

Fig. 5 The time-dependent BL of new derivatives and DeepBlueC™ and coelenterazine in ES-2 cells expressing *Renilla* luciferase (Rluc). (A) Potential compounds that displayed bioluminescence at various cell concentrations; (B) part amplification of (A).

in cellulo compared with coelenterazine. The BL intensity of **B2** is 3 or 4-fold than that of coelenterazine *in cellulo*. Compounds **B5**, **B9** and **B12** display moderate BL emission with 30–40% BL intensity of that of coelenterazine. It is worth noting that the superior BL emission of **B2** could last 40 min compared to coelenterazine in the cellular level (Fig. 5), which indicates that **B2** has the potential to replace coelenterazine as a new outstanding bioluminescent substrate. Compounds **B5**, **B9** and **B12** can emit longer bioluminescence when compared with DeepBlueC™ as shown in Fig. 5B. Moreover, the bioluminescence emission of **B5** could increase and decrease in a slow way, which means that it also has the potential to be used as a probe in a long-time cellular bioluminescence assay. Compound **B12** behaved better *in cellulo* compared to its performance with *Renilla* luciferase. The one reason why they exhibit better performance may be that they have appropriate lipid–water partition coefficients whereas the $C\log P$ of **B2**, coelenterazine and DeepBlueC™ are 4.64, 4.42 and 5.52, respectively (Table S3†). The compound **B2** has better lipid solubility compared to coelenterazine and better water solubility compared to DeepBlueC™, which makes it surpass DeepBlueC™ and coelenterazine. In addition, compounds **B2**, **B5** and **B12** did not influence the cell viability when they were used in the bioluminescence assay (Fig. S2†). As a result, compounds **B2**, **B5**, **B9** and **B12** are potent coelenterazine-type bioluminescence substrates *in vitro* in this research.

Bioluminescence imaging *in vivo*

Encouraged by the results described above, we further investigated the bioluminescence properties of the best performing substrate **B2**, as well as **B5** and **B12**, utilizing the establishment of a nude mice model transplanted with ES-2-Rluc. The *in vivo* bioluminescence imaging results of **B2**, **B5**, **B12** and coelenterazine are depicted in Fig. 6. Whether the compound concentration is 1 mM or 5 mM, the bioluminescence of **B2** is greatly brighter than that of coelenterazine. The BL intensity of **B2** is 4-fold stronger than that of coelenterazine at 1 mM but 6-fold at 5 mM (Fig. 7), which has a significant difference. The bioluminescence of **B2** *in vivo* could last nearly 2 h, which is longer than that of coelenterazine. It is no wonder that compounds **B5** and **B12** exhibit poor performance in bioluminescence imaging

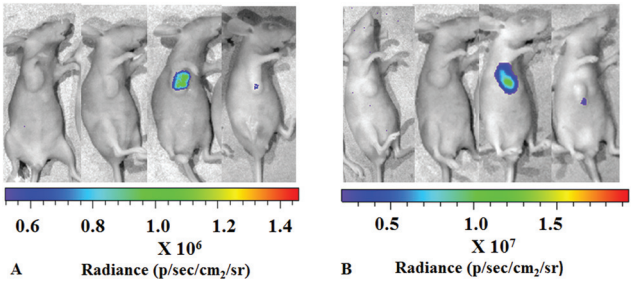

Fig. 6 (A) *In vivo* imaging of **B12**, **B5**, **B2** and coelenterazine at 1 mM in mice bearing tumor xenografts; (B) *in vivo* imaging of **B12**, **B5**, **B2** and coelenterazine at 5 mM in mice bearing tumor xenografts. The representative graphs are chosen from one experiment performed in triplicate.

in vivo compared with **B2** and coelenterazine. Hence, we can draw a conclusion that the compound **B2** is the first-class substrate of Rluc which could be capable of replacing coelenterazine especially in bioluminescence imaging *in vivo*.

The reason why the compound **B2** is the best performing substrate is probably that the introduction of the amino, the election rich group at the C-6 position of the structure core contributes a lot to enhance bioluminescence performance *in vitro* and *in vivo*. The introduction of fluorine as a hydrogen-bonding acceptor also makes contribution for interaction with the residues of luciferase. The polarity of the compound becomes suitable due to the introduction of a polar group. According to a previous study, we knew that the coelenterazine type compounds have the same imidazopyrazinone core that should not be modified. We think that the substituents at the C-6 position of the imidazopyrazinone core are the key to modification. The removal of hydroxyl at the C-2 position doesn't weaken bioluminescence. All in all, our study confirmed that the retention or introduction of polar groups with suitable size at the C-6 position plays a critical role in the improvement of bioluminescence.

Conclusions

We designed and synthesized a series of coelenterazine-type derivatives based on DeepBlueC™, investigated their bioluminescence properties with *Renilla* luciferase, and further demonstrated their applications both *in vitro* and *in vivo*. Compounds **B2**, **B5**, **B6**, **B9** and **B12** displayed decent performance in the bioluminescence assay so as to be able to become candidates of luciferin. It is of great significance that the compound **B2** is superior over coelenterazine: it demonstrated higher bioluminescence intensity, better kinetic characteristics, brighter and longer emission with Rluc *in cellulo* and *in vivo*. The results indicated that the introduction of electron rich groups with suitable size at C-6 could promote the recognition and reaction with luciferase. Moreover, an appropriate lipid–water partition coefficient plays a key role in the cellular bioluminescence and *in vivo* imaging of our new substrates. Together, these new compounds, such as **B2**, **B5** and **B12**, have the potential to act as substantially improved substrates tailored for the bioluminescent system or as a probe to explore some biological process in relevant fields. We hope that our studies provide helpful information for further research and application on the bioluminescent system and bioluminescence imaging.

Experimental section

Materials and instruments

All reagents and solvents available were used as received unless otherwise noted. All reactions were monitored by TLC

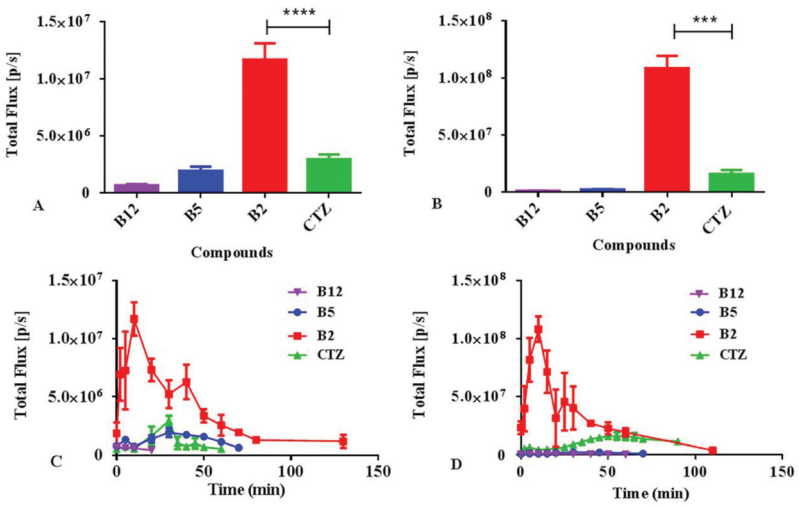

Fig. 7 (A) Quantification of maximum total flux of **B12**, **B5**, **B2** and coelenterazine at 1 mM *in vivo* imaging; (B) quantification of maximum total flux of **B12**, **B5**, **B2** and coelenterazine at 5 mM *in vivo* imaging; (C) time-dependence of compounds **B12**, **B5**, **B2** and coelenterazine at 1 mM *in vivo* imaging; (D) time-dependence of compounds **B12**, **B5**, **B2** and coelenterazine at 5 mM *in vivo* imaging. The error bars are SD for triplicated measurements.

with 0.25 mm silica gel plates (60GF-254). UV light, iodine stain, and ninhydrin were used to visualize the spots. Silica gel was utilized for column chromatography purification. ^{1}H NMR and ^{13}C-NMR were recorded on a Bruker DRX spectrometer at 300 or 400 MHz, δ in parts per million and J in hertz, using TMS as an internal standard. Mass spectra were obtained by using the analytical and the mass spectrometry facilities at Shandong University. HPLC tests were performed with Agilent Technologies 1260 liquid chromatography (Singapore City, Singapore). Melting points were determined uncorrected on an electrothermal melting point apparatus. Water used for the fluorescence and bioluminescence studies was doubly distilled and further purified with a Milli-Q filtration system (Millipore, Watertown, MA, USA). Bioluminescence measurements were determined with an IVIS Kinetic system (Caliper Life Sciences, USA) equipped with a cooled charge-coupled device (CCD) camera or Omega microplate reader (POLARstar Omega, Germany). Bioluminescence spectra were obtained with an F-2500 FL spectrophotometer (Hitachi High Technologies Corporation, Tokyo, Japan). Fluorescence spectra were obtained with a Varioskan microplate spectrophotometer (Thermo Electron Corporation, Waltham, MA, USA). Recombinant *Renilla reniformis* luciferase was purchased from RayBiotech (Norcross, GA, USA). Recombinant *Gaussia* luciferase was purchased from NanoLight (Pinetop, AZ, USA). ES-2 cells (human ovarian cancer cell lines) expressing *Renilla* luciferase (Rluc) were purchased from Shanghai BioDiagnosis Co., Ltd. Coelenterazine was purchased from Chemedir Biopharm-tech. Co., Ltd.

Organic synthesis of new substrates

Preparation of 3-benzyl-5-bromo-2-amino-pyrazine (1).[32,33] Zn dust (235 mg, 3.6 mmol) and I_2 (12 mg) were suspended in fresh anhydrous THF under an argon atmosphere, and the mixture was stirred at room temperature until the brown color of I_2 disappeared. Then the anhydrous benzyl bromide was added by using a syringe, and the reaction mixture was refluxed at 80 °C for 3 h. After insertion of Zn, the reaction mixture was cooled to room temperature. Then the suspension of 2-amino-3,5-dibromopyrazine (506 mg, 2 mmol) and $PdCl_2(PPh_3)_2$ (70 mg, 0.1 mmol) in 7 mL of DMF was added. The reaction mixture was continuously stirred overnight. Then the mixture was filtered by Celatom, and the filtrate was collected and evaporated under vacuum. The collection was dissolved in and extracted with ethyl acetate and washed with saturated sodium chloride solution. After being dried over anhydrous sodium sulfate and concentrated under reduced pressure, the crude product was further purified by chromatography on silica gel (PE/EtOAc 10 : 1) to give a viscous yellow solid (313 mg). Yield: 59%. ^{1}H NMR (400 MHz, DMSO-d_6): δ 7.65 (s, 1H), 7.30–7.25 (m, 5H), 6.56 (s, 1H), 3.98 (s, 2H). ESI-MS: m/z $[M + H]^+$ calcd for 264.01, 266.01, found 264.2, 266.3. Melting point: 73–75 °C.

Preparation of 2-amino-3-benzyl-5-(4-fluorophenyl)-pyrazine (2-1).[32,33] 3-Benzyl-5-bromo-2-amino-pyrazine (500 mg, 1.89 mmol) was added to a suspension of Pd(dppb)Cl_2 (68 mg, 0.11 mmol) and $(C_6H_5CN)_2PdCl_2$ (43 mg, 0.11 mmol) in toluene (6 mL) and stirred at room temperature under an argon atmosphere. 4-Fluorobenzeneboronic acid (397 mg, 2.84 mmol) in toluene (4 mL) and then potassium carbonate aqueous solution (2 M, 0.6 mL) were sequentially added to this mixture with stirring. The mixture was heated to reflux at 109 °C for 8 h and then allowed to cool to room temperature. The mixture was evaporated under vacuum and redissolved in ethyl acetate. Then it was extracted with ethyl acetate and washed with saturated sodium chloride aqueous solution. After being dried over anhydrous sodium sulfate and concentrated under reduced pressure, the crude product was further purified by chromatography on silica gel (PE/EtOAC 20 : 3) to give a white solid (395 mg). Yield: 75%. ^{1}H NMR (400 MHz, DMSO-d_6): δ 8.42 (s, 1H), 7.97–7.93 (m, 2H), 7.3–7.18 (m, 7H), 6.48 (s, 2H), 4.09 (s, 2H). ^{13}C NMR (100 MHz, DMSO): δ 163.5, 161.1, 152.9, 140.9, 138.5, 138.3, 134.1, 129.4, 128.7, 127.2, 127.1, 126.7, 116.1, 115.8, 39.0. ESI-HRMS: m/z $[M + H]^+$ calcd for 280.1250, found 280.1253. Melting point: 126–128 °C.

2-Amino-3-benzyl-5-(4-amino-3-fluorophenyl)-pyrazine (2-2). Yellow solid; yield 60%; ^{1}H NMR (400 MHz, DMSO-d_6): δ 8.31 (s, 1H), 7.54–7.46 (m, 2H), 7.34–7.26 (m, 4H), 7.21–7.17 (m, 1H), 6.80–6.75 (t, J = 10 Hz, 2H), 6.21(s, 2H), 5.26 (s, 2H), 4.04 (s, 2H). ^{13}C NMR (100 MHz, DMSO): δ 152.4, 140.1, 138.7, 136.5, 136.3, 136.2, 129.4, 128.7, 126.6, 121.4, 116.7, 116.6, 111.8, 111.6, 39.1. ESI-HRMS: m/z $[M + H]^+$ calcd for 295.1359, found 295.1340. Melting point: 143–144 °C.

2-Amino-3-benzyl-5-(4-hydroxymethylphenyl)-pyrazine (2-3). Yellow solid; yield 64%; ^{1}H NMR (400 MHz, DMSO-d_6): δ 8.41 (s, 1H), 7.87 (d, J = 8 Hz, 2H), 7.35 (d, J = 8 Hz, 4H), 7.28 (t, J = 8 Hz, 2H), 7.21–7.17 (t, J = 8 Hz, 1H), 6.37 (s, 2H), 5.19 (t, J = 6 Hz, 1H), 4.51 (d, J = 8 Hz, 2H), 4.08 (s, 2H). ^{13}C NMR (100 MHz, DMSO): δ 153.1, 142.2, 140.4, 139.3, 138.6, 137.3, 136.1, 129.4, 128.7, 127.2, 126.6, 125.0, 63.1, 39.1. ESI-HRMS: m/z $[M + H]^+$ calcd for 292.1450, found 292.1454. Melting point: 163–164 °C.

2-Amino-3-benzyl-5-(4-nitrilephenyl)-pyrazine (2-4). Yellow solid; yield 54%; ^{1}H NMR (400 MHz, CD_3OD): δ 8.45 (s, 1H), 8.11 (d, J = 8 Hz, 2H), 7.76 (d, J = 8 Hz, 2H), 7.32–7.23 (m, 5H), 4.16 (s, 2H). ^{13}C NMR (100 MHz, DMSO): δ 152.7, 142.7, 141.6, 138.0, 136.6, 133.2, 129.5, 128.8, 126.8, 125.6, 119.5, 110.1, 38.9. ESI-HRMS: m/z $[M + H]^+$ calcd for 287.1297, found 287.1299. Melting point: 187–189 °C.

2-Amino-3-benzyl-5-(5-methylfuryl)-pyrazine (2-5). Yellow solid; yield 24%; ^{1}H NMR (400 MHz, CD_3OD): δ 8.18 (s, 1H), 7.32–7.21 (m, 5H), 6.71 (d, J = 3.2 Hz, 1H), 6.13 (d, J = 2.4 Hz, 1H), 4.13 (s, 2H), 2.38 (s, 3H). ^{13}C NMR (100 MHz, DMSO): δ 152.8, 151.7, 151.1, 140.7, 138.4, 135.6, 133.5, 129.2, 128.7, 126.7, 108.4, 106.6, 38.9, 13.9. ESI-HRMS: m/z $[M + H]^+$ calcd for 266.1293, found 266.1280. Melting point: 129–130 °C.

2-Amino-3-benzyl-5-(furyl-3)-pyrazine (2-6). Yellow solid; yield 76%; ^{1}H NMR (400 MHz, DMSO-d_6): δ 8.19 (s, 1H), 8.07 (s, 1H), 7.70 (s, 1H), 7.32–7.19 (m, 5H), 6.91 (s, 1H), 6.27 (s, 1H), 4.04 (s, 2H). ^{13}C NMR (100 MHz, DMSO): δ 152.7, 144.5, 140.8, 139.5, 138.5, 136.9, 134.6, 129.3, 128.7, 126.6, 125.0,

108.6, 38.9. ESI-HRMS: m/z $[M + H]^+$ calcd for 252.1137, found 252.1141. Melting point: 130–131 °C.

2-Amino-3-benzyl-5-(3-methoxycarbonylphenyl)-pyrazine (2-7). Yellow solid; yield 74%; ^{1}H NMR (400 MHz, DMSO-d_6): δ 8.50 (d, J = 4 Hz, 2H), 8.19 (d, J = 8 Hz, 1H), 7.88 (d, J = 8 Hz, 1H), 7.56 (t, J = 8 Hz, 1H), 7.31 (m, 4H), 6.55 (s, 2H), 4.11 (s, 2H), 3.88 (s, 3H). ^{13}C NMR (100 MHz, DMSO): δ 166.7, 153.6, 140.7, 138.4, 138.2, 137.9, 137.8, 130.6, 129.6, 129.4, 128.7, 128.3, 126.7, 125.7, 52.7, 39.0. ESI-MS: m/z $[M + H]^+$ calcd for 320.1399, found 320.1408. Melting point: 159–161 °C.

2-Amino-3-benzyl-5-(benzofuranyl-2)-pyrazine (2-8). Yellow solid; yield 37%; ^{1}H NMR (400 MHz, DMSO-d_6): δ 8.41 (s, 1H), 7.65–7.59 (m, 2H), 7.36–7.18 (m, 7H), 6.72 (s, 2H), 4.11 (s, 2H). ^{13}C NMR (100 MHz, DMSO): δ 154.9, 154.6, 153.8, 141.5, 138.2, 137.5, 132.1, 129.3, 129.2, 128.8, 126.8, 124.7, 123.7, 121.4, 111.5, 101.5, 39.0. ESI-HRMS: m/z $[M + H]^+$ calcd for 302.1293, found 302.1293. Melting point: 175–177 °C.

2-Amino-3-benzyl-5-(furyl-2)-pyrazine (2-9). Yellow solid; yield 13%; ^{1}H NMR (400 MHz, DMSO-d_6): δ 8.21 (s, 1H), 7.69 (s, 1H), 7.32–7.18 (m, 5H), 6.74 (d, J = 3.2 Hz, 1H), 6.56 (d, J = 1.2 Hz, 1H), 6.45 (s, 2H), 4.06 (s, 2H). ^{13}C NMR (100 MHz, DMSO): δ 153.0, 152.6, 142.9, 140.9, 138.3, 136.0, 133.2, 129.2, 128.7, 126.7, 112.3, 105.7, 38.9. ESI-HRMS: m/z $[M + H]^+$ calcd for 252.1137, found 252.1138. Melting point: 124–126 °C.

2-Amino-3-benzyl-5-(4-methoxyphenyl)-pyrazine (2-10). Yellow solid; yield 36%; ^{1}H NMR (400 MHz, $CDCl_3$): δ 8.34 (s, 1H), 7.90–7.87 (d, J = 12 Hz, 2H), 7.34–7.24 (m, 5H), 7.01–6.98 (d, J = 12 Hz, 2H), 4.35 (s, 2H), 4.18 (s, 2H), 3.86 (s, 3H). ^{13}C NMR (100 MHz, DMSO): δ 159.4, 152.7, 136.6, 129.4, 128.7, 126.6, 126.5, 114.5, 55.6, 39.1. ESI-HRMS: m/z $[M + H]^+$ calcd for 292.1450, found 292.1452. Melting point: 153–154 °C.

2-Amino-3-benzyl-5-(naphthyl)-pyrazine (2-11). Light brown solid; yield 17%; ^{1}H NMR (400 MHz, DMSO-d_6): δ 8.60 (s, 1H), 8.45 (s, 1H), 8.12 (d, J = 8 Hz, 1H), 7.95 (d, J = 8 Hz, 2H), 7.90 (d, J = 8 Hz, 1H), 7.54–7.48 (m, 2H), 7.38 (d, J = 4 Hz, 2H), 7.31 (t, J = 8 Hz, 2H), 7.21 (t, J = 8 Hz, 1H), 6.55 (s, 2H), 4.15 (s, 2H). ^{13}C NMR (100 MHz, DMSO): δ 153.3, 140.7, 139.0, 138.6, 137.8, 135.1, 133.7, 132.8, 129.4, 128.7, 128.6, 128.6, 128.0, 126.8, 126.7, 126.3, 123.8, 123.4, 39.1. ESI-HRMS: m/z $[M + H]^+$ calcd for 312.1501, found 312.1497. Melting point: 130–132 °C.

2-Amino-3-benzyl-5-(thienyl-2)-pyrazine (2-12). Yellow solid; yield 60%; ^{1}H NMR (400 MHz, DMSO-d_6): δ 8.38 (s, 1H), 7.53–7.07 (m, 8H), 6.43 (s, 2H), 4.04 (s, 2H). ^{13}C NMR (100 MHz, DMSO): δ 153.0, 143.2, 140.3, 138.3, 136.3, 136.2, 129.3, 128.6, 126.7, 125.9, 122.1, 38.7. ESI-HRMS: m/z $[M + H]^+$ calcd for 268.0908, found 268.0907. Melting point: 130–132 °C.

2-Amino-3-benzyl-5-phenyl-pyrazine (2-13). Light brown solid; yield 70%; ^{1}H NMR (400 MHz, $CDCl_3$): δ 8.40 (s, 1H), 7.95 (d, J = 8 Hz, 2H), 7.46 (t, J = 8 Hz, 2H), 7.38–7.26 (m, 6H), 4.41 (s, 2H), 4.20 (s, 2H). ^{13}C NMR (100 MHz, DMSO): δ 153.3, 140.5, 139.2, 138.6, 137.6, 137.5, 129.4, 129.1, 128.7, 127.8, 126.6, 125.2, 39.1. ESI-MS: m/z $[M + H]^+$ calcd for 262.13, found 262.4. Melting point: 142–144 °C.

Preparation of 3-phenyl-1,1-diethoxyacetone (3).[23] Ethyl diethoxyacetate (500 mg, 2.84 mmol) was dissolved in fresh anhydrous THF and the solution was cooled to −78 °C under an argon atmosphere. Then benzylmagnesium chloride (642 mg, 4.26 mmol) solution was added *via* syringe over 15 min, and the reaction was allowed to stir for 3 h. The reaction was quenched by the addition of ammonium chloride aqueous solution and then allowed to warm to room temperature. The reagent was evaporated under vacuum and re-dissolved in ethyl acetate. After extraction with ethyl acetate, the organic layer was washed with saturated sodium chloride aqueous solution. The mixture was concentrated under reduced pressure and then was subjected to chromatography on silica gel (PE/EtOAC 20 : 1) to give a colorless oil (380 mg). Yield: 60%. ^{1}H NMR (400 MHz, DMSO-d_6): δ 7.31–7.16 (m, 6H), 4.80 (s, 1H), 3.87 (s, 2H), 3.66–3.53 (m, 4H). ESI-MS: m/z $[M + NH_4]^+$ calcd for 240.16, found 240.5.

Preparation of 2-benzyl-8-benzyl-6-(4-fluorophenyl)imidazo[1,2-*a*]pyrazin-3(7*H*)-one (B1).[24,32,33] The mixture of 2-amino-3-benzyl-5-(4-fluorophenyl)-pyrazine (**2-1**, 100 mg, 0.35 mmol) and 3-phenyl-1,1-diethoxyacetone (**3-1**, 160 mg, 0.72 mmol) was dissolved in ethanol (3 mL) under an argon atmosphere and allowed to stir at room temperature for 10 min. Conc. HCl (0.2 mL) in ethanol (2 mL) was then added to the mixture *via* syringe over 10 min. The reaction mixture was heated to reflux at 80 °C for 8 h and then allowed to cool to room temperature. The crude was concentrated under vacuum and further purified by chromatography on silica gel (CH_2Cl_2/MeOH 50 : 1) to give a white solid (44 mg). Yield: 30%. Analytical RP HPLC (Phenomenex, C8, 250 × 4.6 mm column): 60% acetonitrile with 0.1% trifluoroacetic acid, 1.0 mL min^{-1} at 370 nm, R_t: 5.315 min, 100%. ^{1}H NMR (400 MHz, CD_3OD): δ 8.58 (s, 1H), 8.02–7.98 (m, 2H), 7.40–7.39 (m, 2H), 7.34–7.22 (m, 10H), 4.55 (s, 2H), 4.30 (s, 2H). ^{13}C NMR (100 MHz, CD_3OD): δ 165.2, 162.7, 136.6, 135.5, 128.9, 128.8, 128.5, 128.4, 128.2, 126.9, 126.8, 115.7, 115.5, 110.1, 37.7, 29.2. ESI-HRMS: m/z $[M + H]^+$ calcd for 410.1669, found 410.1663. Melting point: 195–197 °C.

2-Benzyl-8-benzyl-6-(4-amino-3-fluorophenyl)imidazo[1,2-*a*]pyrazin-3(7*H*)-one (B2). Dark yellow solid; yield 42%; Analytical RP HPLC (Phenomenex, C8, 250 × 4.6 mm column): 60% acetonitrile with 0.1% trifluoroacetic acid, 1.0 mL min^{-1} at 380 nm, R_t: 5.315 min, 97%. ^{1}H NMR (400 MHz, CD_3OD): δ 8.97 (s, 1H), 8.14–8.08 (m, 2H), 7.69 (t, J = 8 Hz, 1H), 7.45–7.26 (m, 10H), 4.62 (s, 2H), 4.38 (s, 2H). ^{13}C NMR (100 MHz, CD_3OD): δ 157.3, 154.9, 148.2, 139.1, 137.9, 136.5, 135.4, 129.1, 128.3, 128.1, 126.9, 126.8, 125.2, 123.3, 123.3, 119.5, 114.8, 114.6, 111.3, 38.2, 28.8. ESI-HRMS: m/z $[M + H]^+$ calcd for 425.1778, found 425.1777. Melting point: 108–110 °C.

2-Benzyl-8-benzyl-6-(4-hydroxymethylphenyl)imidazo[1,2-*a*]pyrazin-3(7*H*)-one (B3). Yellow solid; yield 34%; Analytical RP HPLC (Phenomenex, C8, 250 × 4.6 mm column): 55% acetonitrile with 0.1% trifluoroacetic acid, 1.0 mL min^{-1} at 380 nm, R_t: 10.261 min, 97%. ^{1}H NMR (400 MHz, CD_3OD): δ 7.65 (s, 1H), 7.50–7.18 (m, 14H), 4.67 (s, 2H), 4.44 (s, 2H), 4.20 (s, 2H). ^{13}C NMR (100 MHz, CD_3OD): δ 147.4, 143.5, 139.8, 136.8, 132.5, 129.1, 129.0, 128.7, 128.5, 128.4, 128.3, 127.5, 127.2, 127.1, 126.9, 126.7, 125.3, 125.2, 110.2, 63.2, 37.4, 29.6. ESI-HRMS: m/z $[M + H^+]$ calcd for 422.1869, found 422.1865. Melting point: 141–143 °C.

2-Benzyl-8-benzyl-6-(4-nitrilephenyl)imidazo[1,2-*a*]pyrazin-3(7*H*)-one (B4). Brown solid; yield 39%; Analytical RP HPLC (Phenomenex, C8, 250 × 4.6 mm column): 50% acetonitrile with 0.1% trifluoroacetic acid, 1.0 mL min^{-1} at 380 nm, R_t: 9.776 min, 96%. ^{1}H NMR (400 MHz, CD_3OD): δ 8.88 (s, 1H), 8.23 (d, J = 8 Hz, 2H), 7.86 (d, J = 8 Hz, 2H), 7.42–7.25 (m, 10H), 4.58 (s, 2H), 4.34 (s, 2H). ^{13}C NMR (100 MHz, CD_3OD): δ 150.7, 148.1, 139.7, 139.0, 137.9, 135.5, 132.5, 132.5, 129.1, 128.6, 128.4, 128.2, 127.2, 126.9, 126.9, 121.9, 118.0, 112.7, 111.6, 38.2, 28.8. ESI-HRMS: m/z $[M + H]^+$ calcd for 417.1715, found 417.1717. Melting point: 179–181 °C.

2-Benzyl-8-benzyl-6-(5-methylfuryl)imidazo[1,2-*a*]pyrazin-3(7*H*)-one (B5). Light brown solid; yield 30%; Analytical RP HPLC (Phenomenex, C8, 250 × 4.6 mm column): 55% acetonitrile with 0.1% trifluoroacetic acid, 1.0 mL min^{-1} at 320 nm, R_t: 6.953 min, 99%. ^{1}H NMR (400 MHz, CD_3OD): δ 7.72 (s, 1H), 7.27–7.09 (m, 10H), 6.72 (d, J = 3.2 Hz, 1H), 6.07 (d, J = 2.8 Hz, 1H), 4.31 (s, 2H), 4.07 (s, 2H). ^{13}C NMR (100 MHz, CD_3OD): δ 154.7, 148.1, 147.3, 137.9, 136.6, 135.4, 133.9, 128.9, 128.5, 128.3, 128.2, 126.9, 126.8, 121.9, 111.7, 108.2, 106.7, 37.7, 29.1. ESI-HRMS: m/z $[M + H]^+$ calcd for 396.1712, found 396.1703. Melting point: 185–188 °C.

2-Benzyl-8-benzyl-6-(furyl-3)imidazo[1,2-*a*]pyrazin-3(7*H*)-one (B6). Yellow solid; yield 43%; Analytical RP HPLC (Phenomenex, C8, 250 × 4.6 mm column): 50% acetonitrile with 0.1% trifluoroacetic acid, 1.0 mL min^{-1} at 370 nm, R_t: 4.551 min, 98%. ^{1}H NMR (400 MHz, CD_3OD): δ 8.54 (s, 1H), 8.19 (s, 1H), 7.65 (s, 1H), 7.43 (d, J = 8 Hz, 2H), 7.37–7.23 (m, 8H), 7.02 (d, J = 4 Hz, 1H), 4.58 (s, 2H), 4.34 (s, 2H). ^{13}C NMR (100 MHz, CD_3OD): δ 147.7, 144.5, 142.3, 136.7, 135.5, 128.9, 128.5, 128.3, 128.2, 126.9, 126.7, 121.7, 109.1, 107.7, 37.4, 29.3. ESI-HRMS: m/z $[M + H]^+$ calcd for 382.1556, found 382.1557. Melting point: 191–194 °C.

2-Benzyl-8-benzyl-6-(3-ethyloxycarbonylphenyl)imidazo[1,2-*a*]pyrazin-3(7*H*)-one (B7). Dark yellow solid; yield 31%; Analytical RP HPLC (Phenomenex, C8, 250 × 4.6 mm column): 45% acetonitrile with 0.1% trifluoroacetic acid, 1.0 mL min^{-1} at 370 nm, R_t: 6.564 min, 98%. ^{1}H NMR (400 MHz, CD_3OD): δ 8.78 (s, 1H), 8.65 (s, 1H), 8.23 (d, J = 8 Hz, 1H), 8.07 (d, J = 8 Hz, 1H), 7.46 (d, J = 4 Hz, 2H), 7.39–7.24 (m, 9H), 4.61 (s, 2H), 4.42 (q, J = 8 Hz, 2H), 4.40–4.34 (m, 2H), 1.43 (t, J = 8 Hz, 3H). ^{13}C NMR (100 MHz, CD_3OD): δ 166.2, 150.4, 147.8, 140.1, 138.0, 136.6, 135.5, 134.8, 130.8, 129.0, 128.6, 128.4, 128.2, 126.9, 126.8, 110.6, 61.2, 37.9, 29.1, 13.3. ESI-HRMS: m/z $[M + H]^+$ calcd for 464.1974, found 464.1964. Melting point: 188–190 °C.

2-Benzyl-8-benzyl-6-(benzofuranyl-2)imidazo[1,2-*a*]pyrazin-3(7*H*)-one (B8). Dark yellow solid; yield 58%; Analytical RP HPLC (Phenomenex, C8, 250 × 4.6 mm column): 45% acetonitrile with 0.1% trifluoroacetic acid, 1.0 mL min^{-1} at 380 nm, R_t: 6.564 min, 98%. ^{1}H NMR (400 MHz, CD_3OD): δ 8.55 (s, 1H), 7.57 (t, J = 6 Hz, 4H), 7.47 (d, J = 8 Hz, 3H), 7.31 (t, J = 8 Hz, 4H), 7.24 (m, 3H), 7.13 (s, 1H), 4.63 (s, 2H), 4.36 (s, 2H). ^{13}C NMR (100 MHz, CD_3OD): δ 155.0, 151.5, 149.1, 138.0, 137.7, 136.7, 132.8, 129.9, 129.1, 129.0, 128.9, 128.7, 128.4, 127.4, 127.3, 127.1, 126.4, 124.1, 122.3, 120.5, 111.8, 110.3, 106.7, 100.0, 38.1, 29.2. ESI-HRMS: m/z $[M + H]^+$ calcd for 432.1712, found 432.1703. Melting point: 207–209 °C.

2-Benzyl-8-benzyl-6-(furyl-2)imidazo[1,2-*a*]pyrazin-3(7*H*)-one (B9). Dark yellow solid; yield 30%; Analytical RP HPLC (Phenomenex, C8, 250 × 4.6 mm column): 50% acetonitrile with 0.1% trifluoroacetic acid, 1.0 mL min^{-1} at 370 nm, R_t: 4.586 min, 98%. ^{1}H NMR (400 MHz, CD_3OD): δ 8.50 (s, 1H), 7.69 (s, 1H), 7.43–7.27 (m, 10H), 7.08 (d, J = 4 Hz, 1H), 6.60 (s, 1H), 4.56 (s, 2H), 4.34 (s, 2H). ^{13}C NMR (100 MHz, CD_3OD): δ 149.2, 148.2, 144.3, 138.0, 136.5, 135.4, 134.0, 128.6, 128.3, 128.1, 121.0, 111.9, 110.5, 107.6, 37.8, 29.0. ESI-HRMS: m/z $[M + H]^+$ calcd for 382.1556, found 382.1545. Melting point: 184–186 °C.

2-Benzyl-8-benzyl-6-(4-methoxyphenyl)imidazo[1,2-*a*]pyrazin-3(7*H*)-one (B10). Yellow solid; yield 52%; Analytical RP HPLC (Phenomenex, C8, 250 × 4.6 mm column): 55% acetonitrile with 0.1% trifluoroacetic acid, 1.0 mL min^{-1} at 370 nm, R_t: 7.431 min, 98%. ^{1}H NMR (400 MHz, CD_3OD): δ 7.91 (s, 1H), 7.68–7.66 (d, J = 8 Hz, 2H), 7.40–7.38 (d, J = 8 Hz, 2H), 7.32–7.17 (m, 8H), 7.04–7.02 (d, J = 8 Hz, 2H), 4.46 (s, 2H), 4.21 (s, 2H), 3.83 (s, 3H). ^{13}C NMR (100 MHz, CD_3OD): δ 161.4, 139.6, 138.4, 136.8, 135.6, 128.9, 128.5, 128.4, 128.2, 128.2, 126.9, 126.7, 125.8, 114.2, 109.3, 54.6, 37.4, 29.7. ESI-HRMS: m/z $[M + H]^+$ calcd for 422.1869, found 422.1863. Melting point: 184–187 °C.

2-Benzyl-8-benzyl-6-(naphthyl)imidazo[1,2-*a*]pyrazin-3(7*H*)-one (B11). Dark yellow solid; yield 12%; Analytical RP HPLC (Phenomenex, C8, 250 × 4.6 mm column): 63% acetonitrile with 0.1% trifluoroacetic acid, 1.0 mL min^{-1} at 395 nm, R_t: 4.547 min, 96%. ^{1}H NMR (400 MHz, CD_3OD): δ 8.76 (s, 1H), 8.52 (s, 1H), 8.00 (m, 4H), 7.56–7.11 (m, 14H), 4.62 (s, 2H), 4.34 (s, 2H). ^{13}C NMR (100 MHz, CD_3OD): δ 150.01, 145.43, 144.34, 139.60, 135.09, 133.67, 131.44, 129.69, 129.21, 129.05, 128.55, 128.41, 128.38, 128.32, 128.25, 128.17, 127.33, 126.96, 126.82, 126.55, 126.35, 124.93, 124.66, 122.39, 120.53, 38.52, 22.11. ESI-HRMS: m/z $[M + H]^+$ calcd for 442.1919, found 442.1915. Melting point: 117–119 °C.

2-Benzyl-8-benzyl-6-(thienyl-2)imidazo[1,2-*a*]pyrazin-3(7*H*)-one (B12). Yellow solid; yield 50%; Analytical RP HPLC (Phenomenex, C8, 250 × 4.6 mm column): 50% acetonitrile with 0.1% trifluoroacetic acid, 1.0 mL min^{-1} at 380 nm, R_t: 8.969 min, 96%. ^{1}H NMR (400 MHz, DMSO): δ 8.71 (s, 1H), 7.86 (d, J = 4 Hz, 1H), 7.64 (dd, J = 8 Hz, J = 4 Hz, 1H), 7.49–7.17 (m, 11H), 4.49 (s, 2H), 4.26 (s, 2H). ^{13}C NMR (100 MHz, DMSO): δ 147.25, 139.20, 136.82, 136.49, 135.76, 128.77, 128.10, 128.03, 127.93, 127.76, 126.20, 126.12, 125.06, 124.60, 108.02, 37.17, 28.03. ESI-HRMS: m/z $[M + H]^+$ calcd for 398.1327, found 398.1327. Melting point: 261–265 °C.

2-Benzyl-8-benzyl-6-(phenyl)imidazo[1,2-*a*]pyrazin-3(7*H*)-one (B13, DeepBlueC™). Light brown solid; yield 60%; Analytical RP HPLC (Phenomenex, C8, 250 × 4.6 mm column): 50% acetonitrile with 0.1% trifluoroacetic acid, 1.0 mL min^{-1} at 380 nm, R_t: 9.824 min, 97%. ^{1}H NMR (400 MHz, CD_3OD): δ 7.90 (s, 1H), 7.55–7.17 (m, 15H), 4.37 (s, 2H), 4.11 (s, 2H). ^{13}C NMR (100 MHz, CD_3OD): δ 147.9, 139.6, 138.0, 137.8, 136.8, 136.7, 134.5, 130.1, 129.8, 129.5, 129.1, 129.0, 128.9,

127.4, 127.2, 127.0, 126.4, 111.2, 38.0, 29.5. ESI-HRMS: m/z $[M + H]^+$ calcd for 392.1763, found 392.1755. Melting point: 259–261 °C.

Bioluminescence assay

Millipore water was used to prepare all aqueous solutions. Measurements for *Renilla* luciferase bioluminescent assays were determined in 50 mM Tris-HCl buffer, pH 7.42. Measurements for *Gaussia* luciferase bioluminescent assays were determined in 25 mM Tris-HCl buffer, pH 7.8, with 600 mM NaCl, 1 mM EDTA, and 0.05% BSA. The bioluminescence images were captured by using an IVIS Kinetic system (Caliper Life Sciences, USA) equipped with a cooled charge-coupled device (CCD) camera. The bioluminescence spectra were recorded on an F-2500 fluorescence spectrophotometer in luminescence mode. Luciferase was purchased from RayBiotech. The bioluminescence kinetic parameters, including K_m, V_{max} and half decay life, were calculated using GraphPad Prism software.

Bioluminescence properties measurement (*Renilla* luciferase)

To determine the bioluminescence properties of the new derivatives, all compounds were freshly dissolved in 95% EtOH as stock and diluted to appropriate concentrations in Tris-HCl (50 mM, pH 7.42) for each measurement. In all the measurements, the final ethanol concentration in the sample solution was kept constant at 0.5% (v/v) to avoid the effect of ethanol on the BL reaction. The *Renilla* luciferase was dissolved in and diluted to 1 μg ml^{-1} with Tris-HCl (50 mM, pH 7.42). To measure the bioluminescence intensity, the solution of the compound (50 μL) was added to a 96-well black flat bottom microscale plate, and luciferase (50 μL) was added and mixed quickly. The final concentration of luciferase was 0.5 μg mL^{-1}. The final compound concentrations were 0.25, 0.5, 1, 2, 5, 10 and 25 μM. Bioluminescence intensities of native coelenterazine and the derivatives were immediately measured with an IVIS Kinetic system (Caliper Life Sciences, USA) equipped with a cooled charge-coupled device (CCD) camera. The assays were measured in triplicate. The results were reported as total photon flux within an ROI in photons per second. The Michaelis constant K_m and maximum rate V_{max} were estimated with the Michaelis–Menten kinetics equation using GraphPad Prism software.

For the recording of bioluminescence spectra, an aliquot of *Renilla* luciferase solution (0.5 mL, 1 μg mL^{-1}) was mixed with derivative solution (0.5 mL, 25 μM) in a quartz cell and the mixture was immediately measured with an F-2500 fluorescence spectrophotometer in luminescence wavelength mode with the lamp off at a scan rate of 3000 nm min^{-1} with a response time of 2 s. The wavelengths of maximal bioluminescence intensities (λ_{max}) and the quantitative bioluminescence spectra were determined using the instrument software (FL Solutions ver. 2.1).

In the case of determining the half decay life, an aliquot of *Renilla* luciferase solution (0.5 mL, 1 μg mL^{-1}) was mixed with derivative solution (0.5 mL, 25 μM) in a quartz cell and the mixture was immediately measured with an F-2500 fluorescence spectrophotometer in luminescence time scan mode with the lamp off at a scan rate of 3000 nm min^{-1} with a response time of 2 s. The measurement lasted 300 s. The half decay life was calculated by using GraphPad Prism software.

Bioluminescence properties measurement (*Gaussia* luciferase)

To determine the bioluminescence properties of the new derivatives, all compounds were freshly dissolved in 95% EtOH as stock and diluted to appropriate concentrations in Tris-HCl (25 mM, pH 7.8, containing 600 mM NaCl, 1 mM EDTA, 0.05% BSA) for each measurement. In all the measurements, the final ethanol concentration in the sample solution was kept constant at 0.5% (v/v) to avoid the effect of ethanol on the BL reaction. The *Gaussia* luciferase was dissolved in and diluted to 0.5 μg mL^{-1} with Tris-HCl (25 mM, pH 7.8, containing 600 mM NaCl, 1 mM EDTA, 0.05% BSA). To measure the bioluminescence intensity, the solution of the compound (50 μL) was added to a 96-well black flat bottom microscale plate, and luciferase (50 μL) was added and mixed quickly. The final concentration of luciferase was 0.25 μg mL^{-1}. The final compound concentrations were 0.25, 0.5, 1, 2, 5, 10 and 25 μM. Bioluminescence intensities of native coelenterazine and the derivatives were immediately measured with a POLARstar Omega microplate reader. The assays were measured in triplicate. The Michaelis constant K_m and maximum rate V_{max} were estimated with the Michaelis–Menten kinetics equation using GraphPad Prism software.

For the recording of bioluminescence spectra, an aliquot of *Gaussia* luciferase solution (0.5 mL, 0.5 μg mL^{-1}) was mixed with derivative solution (0.5 mL, 25 μM) in a quartz cell and the mixture was immediately measured with an F-2500 fluorescence spectrophotometer in luminescence wavelength mode with the lamp off at a scan rate of 3000 nm min^{-1} with a response time of 2 s. The wavelengths of maximal bioluminescence intensities (λ_{max}) and the quantitative bioluminescence spectra were determined using the instrument software (FL Solutions ver. 2.1).

In the case of recording half decay life, the solution of the compound (50 μL) was added to a 96-well black flat bottom microscale plate, and luciferase (50 μL) was added and mixed quickly and was immediately measured with a POLARstar Omega microplate reader with a measurement time of 300 s. The half decay life was calculated by using GraphPad Prism software.

Cell culture

ES-2 cells (human ovarian cancer cell lines) expressing *Renilla* luciferase (Rluc) were purchased from Shanghai BioDiagnosis Co., Ltd. The ES-2-Rluc cells were cultured in DMEM high glucose supplemented with 10% fetal bovine serum (FBS) at 37 °C under a humidified atmosphere in a 5% CO_2 incubator.

Cell bioluminescence imaging

Cells were grown in black 96-well plates (4×10^5 cells per well). After a 24 h incubation period, the medium was removed, and

the cells were treated with 100 μL of various concentrations of compounds (ranging from 0.25 to 25 μM). The bioluminescence intensity was measured immediately using an IVIS Kinetic imaging system. The luminescent signal (photons per second) for each well was measured and plotted as average values (experiments conducted in triplicate).

Cell concentration-dependent assay

Cells were grown in black 96-well plates (0.125, 0.25, 0.5, 1, 2 and 4×10^5 cells per well, respectively). After a 24 h incubation period, the medium was removed, and the cells were treated with 100 μL of compounds (50 μM). The bioluminescence intensity was measured immediately using an IVIS Kinetic imaging system. The luminescent signal (photons per second) for each well was measured and plotted as average values (experiments conducted in triplicate).

Cytotoxicity of new coelenterazine derivatives

The cytotoxicity of the new coelenterazine derivatives **B2**, **B9** and **B12** was investigated in ES-2-Rluc cells. ES-2-Rluc cells were grown overnight at 5000 per well in DMEM with 10% FBS. Then the new coelenterazine derivatives (or DMSO control) that were diluted in DMEM were added into the wells. MTT was added 2 h after compound addition. Cell viability was measured 4 h after MTT addition by using a POLARstar Omega microplate reader.

Mice model

All animal studies were approved by the Ethics Committee and IACUC of Qilu Health Science Center, Shandong University, and were conducted in compliance with European Guidelines for the Care and Use of Laboratory Animals. Balb/c-nu female mice, 6 weeks of age, were purchased from the Animal Center of China Academy of Medical Sciences (Beijing, China). To generate tumor xenografts in mice, ES-2 cells expressing *Renilla* luciferase (1×10^7) were implanted subcutaneously under the right armpit region of each 6 weeks old female nude mouse. Mice were single or group-housed on a 12 : 12 light–dark cycle at 22 °C with free access to food and water. Tumors were allowed to grow for 2 weeks before imaging.

In vivo imaging

New substrates **B2**, **B5** and **B12** were chosen for bioluminescence imaging in mice. All compounds were freshly dissolved in and diluted to appropriate concentrations in 0.9% NaCl and 95% EtOH (3 : 1 v/v) for this measurement. To demonstrate this functionality, mice bearing ES-2-Rluc subcutaneous tumors were anesthetized with isoflurane and then were injected intraperitoneally with a solution of the compound (100 μL). The bioluminescence was detected at once with an exposure time of 60 s.

Chemiluminescence spectra measurement

All compounds were freshly dissolved in EtOH as 1 mM solution. A 0.2 mL of compound solution was mixed with 2 mL of DMSO containing 0.05% (v/v) 1 M aq. NaOH in a quartz cell and the mixture was immediately measured with an F-2500 fluorescence spectrophotometer in luminescence mode with the lamp off at a scan rate of 3000 nm min^{-1} with a response time of 2 s. The wavelengths of maximal chemiluminescence intensities (λ_{max}) and the quantitative chemiluminescence spectra were determined using the instrument software (FL Solutions ver. 2.1).

Fluorescence spectra measurement

A 95% ethanol stock solution of the respective new substrate (10 mM) was diluted to the corresponding concentration with Tris-HCl (50 mM, pH 7.42). The solution of the compound (100 μM, 200 μL) was added to a 96-well black flat bottom microscale plate and then scanned with the Thermo Scientific Varioskan Flash microplate reader.

Acknowledgements

This work was supported by grants from the National Program on Key Basic Research Project (no. 2013CB734000), the National Natural Science Foundation of China (no. 81673393), the Taishan Scholar Program at Shandong Province, the Qilu Scholar Program at Shandong University, the American Cancer Society (no. RSG-16-215-01 TBE), the Russian Science Foundation (no. 17-14-01169) and the Major Project of Science and Technology of Shandong Province (no. 2015ZDJS04001).

Notes and references

1 J. Li, L. Chen, W. Wu, W. Zhang, Z. Ma, Y. Cheng, L. Du and M. Li, *Anal. Chem.*, 2014, **86**, 2747–2751.
2 T. Jiang, B. Ke, H. Chen, W. Wang, L. Du, K. Yang and M. Li, *Anal. Chem.*, 2016, **88**, 7462–7465.
3 B. Ke, W. Wu, W. Liu, H. Liang, D. Gong, X. Hu and M. Li, *Anal. Chem.*, 2016, **88**, 592–595.
4 B. Ke, W. Wu, L. Wei, F. Wu, G. Chen, G. He and M. Li, *Anal. Chem.*, 2015, **87**, 9110–9113.
5 W. Wu, J. Li, L. Chen, Z. Ma, W. Zhang, Z. Liu, Y. Cheng, L. Du and M. Li, *Anal. Chem.*, 2014, **86**, 9800–9806.
6 S. H. Haddock, M. A. Moline and J. F. Case, *Annu. Rev. Mar. Sci.*, 2010, **2**, 443–493.
7 O. Shimomura, *Bioluminescence: Chemical Principles and Methods*, World Scientific Publishing Co. Pte. Ltd, 2006.
8 S. Inouye, R. Iimori, Y. Sahara, S. Hisada and T. Hosoya, *Anal. Biochem.*, 2010, **407**, 247–252.
9 O. Shimomura, *Biochem. J.*, 1995, **306**(Pt 2), 537–543.
10 S. Inouye and Y. Sahara, *Biochem. Biophys. Res. Commun.*, 2008, **365**, 96–101.
11 P. Herring, *Hydrobiologia*, 1988, **167–168**, 183–195.
12 M. R. Bowlby and J. F. Case, *Mar. Biol.*, 1991, **110**, 329–336.
13 J. Woo, M. H. Howell and A. G. von Arnim, *Protein Sci.*, 2008, **17**, 725–735.

14 T. Jiang, L. Du and M. Li, *Photochem. Photobiol. Sci.*, 2016, **15**, 466–480.
15 G. A. Stepanyuk, Z.-J. Liu, S. S. Markova, L. A. Frank, J. Lee, E. S. Vysotski and B.-C. Wang, *Photochem. Photobiol. Sci.*, 2008, **7**, 442–447.
16 K. Teranishi, *Bioorg. Chem.*, 2007, **35**, 82–111.
17 S. Inouye and O. Shimomura, *Biochem. Biophys. Res. Commun.*, 1997, **233**, 349–353.
18 C. Wu, H. Nakamura, A. Murai and O. Shimomura, *Tetrahedron Lett.*, 2001, **42**, 2997–3000.
19 G. Giuliani, P. Molinari, G. Ferretti, A. Cappelli, M. Anzini, S. Vomero and T. Costa, *Tetrahedron Lett.*, 2012, **53**, 5114–5118.
20 R. Nishihara, H. Suzuki, E. Hoshino, S. Suganuma, M. Sato, T. Saitoh, S. Nishiyama, N. Iwasawa, D. Citterio and K. Suzuki, *Chem. Commun.*, 2015, **51**, 391–394.
21 M. Yuan, X. Ma, T. Jiang, C. Zhang, H. Chen, Y. Gao, X. Yang, L. Du and M. Li, *Org. Biomol. Chem.*, 2016, **14**, 10267–10274.
22 E. P. Coutant and Y. L. Janin, *Chem. – Eur. J.*, 2015, **21**, 17158–17171.
23 E. Lindberg, S. Mizukami, K. Ibata, T. Fukano, A. Miyawaki and K. Kikuchi, *Chem. Sci.*, 2013, **4**, 4395–4400.
24 E. Lindberg, S. Mizukami, K. Ibata, A. Miyawaki and K. Kikuchi, *Chem. – Eur. J.*, 2013, **19**, 14970–14976.
25 G. A. Stepanyuk, J. Unch, N. P. Malikova, S. V. Markova, J. Lee and E. S. Vysotski, *Anal. Bioanal. Chem.*, 2010, **398**, 1809–1817.
26 J. Levi, A. De, Z. Cheng and S. S. Gambhir, *J. Am. Chem. Soc.*, 2007, **129**, 11900–11901.
27 T. Jiang, X. Yang, X. Yang, M. Yuan, T. Zhang, H. Zhang and M. Li, *Org. Biomol. Chem.*, 2016, **14**, 5272–5281.
28 K. Hori, J. E. Wampler, J. C. Matthews and M. J. Cormier, *Biochemistry*, 1973, **12**, 4463–4468.
29 K. Hori, J. M. Anderson, W. W. Ward and M. J. Cormier, *Biochemistry*, 1975, **14**, 2371–2376.
30 M. P. Hall, J. Unch, B. F. Binkowski, M. P. Valley, B. L. Butler, M. G. Wood, P. Otto, K. Zimmerman, G. Vidugiris, T. Machleidt, M. B. Robers, H. A. Benink, C. T. Eggers, M. R. Slater, P. L. Meisenheimer, D. H. Klaubert, F. Fan, L. P. Encell and K. V. Wood, *ACS Chem. Biol.*, 2012, **7**, 1848–1857.
31 A. M. Loening, T. D. Fenn and S. S. Gambhir, *J. Mol. Biol.*, 2007, **374**, 1017–1028.
32 M. Adamczyk, D. D. Johnson, P. G. Mattingly, Y. Pan and R. E. Reddy, *Org. Prep. Proced. Int.*, 2001, **33**, 477–485.
33 M. Adamczyk, S. R. Akireddy, D. D. Johnson, P. G. Mattingly, Y. Pan and R. E. Reddy, *Tetrahedron*, 2003, **59**, 8129–8142.